Journal of Inorganic Biochemistry 105 (2011) 241–249

Contents lists available at ScienceDirect

Journal of Inorganic Biochemistry

journal homepage: www.elsevier.com/locate/jinorgbio

DNA interaction and cytotoxicity studies of new ruthenium(II) cyclopentadienyl derivative complexes containing heteroaromatic ligands

Virtudes Moreno [a,*], Mercè Font-Bardia [b], Teresa Calvet [b], Julia Lorenzo [c], Francesc X. Avilés [c], M. Helena Garcia [d], Tânia S. Morais [d], Andreia Valente [d], M. Paula Robalo [e]

[a] Department de Química Inorgànica, Universitat de Barcelona, Martí y Franquès 1-11, 08028, Barcelona, Spain
[b] Cristal.lografia, Mineralogia i Dipòsits Minerals, Universitat de Barcelona, Martí y Franquès s/n, 08028, Barcelona, Spain
[c] Departamento de Engenharia Química, Instituto Superior de Engenharia de Lisboa, Rua Conselheiro Emídio Navarro, 1, 1959-007 Lisboa, Centro de Química Estrutural, Complexo I, IST, Av. Rovisco Pais, 1049-001 Lisboa, Portugal
[d] Centro de Ciências Moleculares e Materiais, Faculdade de Ciências da Universidade de Lisboa, Campo Grande, 1749-016 Lisboa, Portugal
[e] Institut de Biotecnologia i de Biomedicina, Universitat Autònoma de Barcelona, 08193, Bellaterra, Barcelona, Spain

ARTICLE INFO

Article history:
Received 18 February 2010
Received in revised form 19 October 2010
Accepted 20 October 2010
Available online 29 October 2010

Keywords:
Ruthenium (II)
Cyclopentadienyl derivatives
X-ray structures
Antiproliferative assays

ABSTRACT

Four ruthenium(II) complexes with the formula $[Ru(\eta^5\text{-}C_5H_5)(PP)L][CF_3SO_3]$, being (PP = two triphenylphosphine molecules), L = 1-benzylimidazole, **1**; (PP = two triphenylphosphine molecules), L = 2,2′bipyridine, **2**; (PP = two triphenylphosphine molecules), L = 4-Methylpyridine, **3**; (PP = 1,2-bis(diphenylphosphine) ethane), L = 4-Methylpyridine, **4**, were prepared, in view to evaluate their potentialities as antitumor agents. The compounds were completely characterized by NMR spectroscopy and their crystal and molecular structures were determined by X-ray diffraction. Electrochemical studies were carried out giving for all the compounds quasi-reversible processes. The images obtained by atomic force microscopy (AFM) suggest interaction with pBR322 plasmid DNA. Measurements of the viscosity of solutions of free DNA and DNA incubated with different concentrations of the compounds confirmed this interaction. The cytotoxicity of compounds **1234** was much higher than that of cisplatin against human leukemia cancer cells (HL-60 cells). IC_{50} values for all the compounds are in the range of submicromolar amounts. Apoptotic death percentage was also studied resulting similar than that of cisplatin.

1. Introduction

In the recent years the research on ruthenium compounds in view to their cytotoxic properties has increased, motivated by the promising results already obtained in both inorganic and organometallic fields where the cytotoxicity reported for some of the compounds is comparable or even better than that of cisplatin [1–3].

Additionally, the finding that the ruthenium(III) coordination compounds, [ImH][trans-$RuCl_4$(DMSO)Im], NAMI-A and (Hind)[trans-$RuCl_4(ind)_2$], KP1019, (ImH = imidazolium, Hind = indazolium) currently in clinical trials [4,5], display very high activity against metastases and the organometallic ruthenium (II) derivative $[Ru(\eta^6\text{-toluene})(pta)Cl_2]$ (RAPTA-T), (pta = 1,3,5-triaza-7-phosphaadamantane) exhibit similar antitumor behavior [6–10], brings additional interest to the ruthenium chemistry for the development of metal-based chemotherapeutics.

A significant number of half sandwich Ru(II)-η^6arene complexes exhibiting antitumor properties against a wide variety of tumor types has been published [11–15] being, some of the complexes, effective against tumor cell lines that are resistant to treatment with cisplatin. Concerning the related isoelectronic "$Ru(\eta^5\text{-}C_5H_5)$" derivatives, only few studies have been reported in the literature; compound $[RuCp^*Cl(pta)_2]$ was tested on TS/A murine adenocarcinoma tumor cells [16] and some compounds derived of the fragment "CpRu(CO)" with pyridocarbazole ligands were found potent and selective inhibitors for protein kinases GSK-3 and Pim-1 [17].

Recently, we start to report our studies on a new family of cationic complexes of general formula $[RuCp(PP)L]^+$ where L is a nitrogen sigma bonded ligand, that showed interaction with DNA by atomic force microscopy and also significant inhibition of the growth of LoVo human colon adenocarcinoma and Mia PaCa pancreatic cell lines [18]. Besides, our tests for potential antitumor activity against the human promyelocytic leukemia cell line HL-60 using a MTT (3-(4,5-dimethylthiazol-2-yl)-2,5-diphenyltetrazolium bromide) assay, were very encouraging revealing excellent antitumor activities, with IC_{50} values lower than that of cisplatin [19].

Our strategy on this field lead us to continue the exploitation of the cytotoxic properties of compounds of general formula $[Ru(\eta^5\text{-}C_5H_5)(PP)L]^+$ where L is a N heteroaromatic sigma bonded ligand, chosen preferentially within planar molecules, in order to potentiate also their intercalation in DNA, besides their possible covalent binding to

* Corresponding author. Tel.: +34 93 4021274; fax: +34 93 4907725.
E-mail address: virtudes.moreno@qi.ub.es (V. Moreno).

0162-0134/$ – see front matter © 2010 Elsevier Inc. All rights reserved.
doi:10.1016/j.jinorgbio.2010.10.009

N7 guanine residues. The present investigation focuses on different hapticity of L which can be monodentate, such as 1-benzylimidazole (1-BI) and 4-methylpyridine (4-Mpy) or occupy two coordination sites, 2,2′-bipyridyl (2,2′-bipy), leading eventually to a different mechanism of action of the complexes. The compounds with 4-Mpy had the variation on the mono and bidentate phosphine coligands to see whether this is a significant variable in the cytotoxicity of the ruthenium complexes. The interaction of these new four compounds with the plasmid pBR322 DNA was studied by AFM, electrophoretical mobility and viscosity measurements, and their cytotoxicity was examined on human leukemia cancer cells (HL-60).

2. Materials and methods

Syntheses were carried out under dinitrogen atmosphere using current Schlenk techniques and the solvents used were dried by standard methods [20]. Starting materials [Ru(η^5-C_5H_5)(PP)Cl] were prepared following the methods described in literature: PP = $2PPh_3$ [21] and dppe [22]. FT-IR spectra were recorded in a Mattson Satellite FT-IR spectrophotometer with KBr; only significant bands are cited in text. ^{1}H, ^{13}C and ^{31}P NMR spectra were recorded on a Bruker Avance 400 spectrometer at probe temperature. The ^{1}H and ^{13}C chemical shifts are reported in parts per million (ppm) downfield from internal Me_4Si and the ^{31}P NMR spectra are reported in ppm downfield from external standard, 85% H_3PO_4. Elemental analyses were obtained at Laboratório de Análises, Instituto Superior Técnico, using a Fisons Instruments EA1108 system. Data acquisition, integration and handling were performed using a PC with the software package EAGER-200 (Carlo Erba Instruments). Electronic spectra were recorded at room temperature on a Jasco V-560 spectrometer in the range of 200–900 nm.

2.1. DNA interaction studies

2.1.1. Formation of drug–DNA complexes

Deionised Milli-Q water (18.2 MΩ) was filtered through 0.2-nm FP030/3 filters (Schleicher & Schuell) and centrifuged at 4.000 *g* prior to use. pBR322 DNA was heated at 60 °C for 10 min to obtain open circular (OC) form. To stock aqueous solutions of plasmid pBR322 DNA in Hepes (2-[4-(2-hydroxyethyl)piperazin-1-yl]ethanesulfonic acid) buffer (4 mM Hepes, pH 7.4/2 mM $MgCl_2$) were added aqueous solutions (with 4% of DMSO) of complexes **1**, **2**, **3** and **4** in a relationship DNA base pair to complex 10:1. In parallel experiments, blank sample of free DNA and DNA complex solutions were equilibrated at 37 °C for 4 h in the dark shortly thereafter.

2.1.2. AFM imaging

Atomic force microscopy (AFM) samples were prepared by casting a 3-μL drop of test solution onto freshly cleaved Muscovite green mica disks as support. The drop was allowed to stand undisturbed for 3 min to favour the adsorbate–substrate interaction. Each DNA-laden disk was rinsed with Milli-Q water and was blown dry with clean compressed argon gas directed normal to the disk surface. Samples were stored over silica prior to AFM imaging. All AFM observations were made with a Nanoscope III Multimode AFM (Digital Instrumentals, Santa Barbara, CA). Nano-crystalline Si cantilevers of 125-nm length with a spring constant of 50 N/m average ended with conical-shaped Si probe tips of 10-nm apical radius and cone angle of 35° were utilized. High-resolution topographic AFM images were performed in air at room temperature (relative humidity<40%) on different specimen areas of 2×2 μm operating in intermittent contact mode at a rate of 1–3 Hz.

2.1.3. Viscosity measurements

Viscosity experiments were carried out with an AND-SV-1 viscometer in a water bath using a water jacket accessory and maintained the constant temperature at 25 °C. Calculated amounts of solutions of the different compounds were added in 2 mL of 100 mM ct-DNA solution in order to achieve the concentrations required.

2.2. Growth inhibition assays

Antiproliferative activity of the ruthenium complexes, and cisplatin, was tested in a cell culture system using the human acute promyelocytic leukemia cell line HL-60 (American Type Culture Collection (ATCC)). The cells were grown in RPMI-1640 medium supplemented with 10% (v/v) heat inactivated fetal bovine serum, 2 mmol/L glutamine, (Invitrogen, Inc.) in a highly humidified atmosphere of 95% air with 5% CO_2 at 37 °C. Growth inhibitory effect was measured by the microculture tetrazolium [3-(4,5-dimethylthiazol-2-yl)-2,5-diphenyl-tetrazolium bromide,MTT] assay [23]. Following the addition of different complex concentrations to quadruplicate wells, plates were incubated at 37 °C for 24 or 72 h. Aliquots of 20 μL of MTT solution were then added to each well. After 3 h, the colour formed was quantitated by a spectrophotometric plate reader (Labsystems iEMS Reader MF) at 490 nm wavelength. Cytotoxicity was evaluated in terms of cell growth inhibition in treated cultures versus that in untreated controls. $IC_{50,}$ the concentration of compound at which cell proliferation was 50% of that observed in control cultures, were obtained by GraphPad Prism software, version 4.0. Experiments were repeated at least three times to get the mean values.

2.3. Apoptosis assays

Induction of apoptosis *in vitro* by ruthenium compounds was determined by a flow cytometric assay with Annexin V-FITC by using an Annexin V-FITC Apoptosis Detection Kit (Roche) [24]. Exponentially growing HL-60 cells in 6-well plates ($5x10^5$cells/well) were exposed to concentrations equal to the IC_{50} of the platinum and ruthenium drugs for 24 h. After, the cells were subjected to staining with the Annexin V-FITC and propidium iodide. The amount of apoptotic cells was analyzed by flow cytometry (BD FACSCalibur).

2.4. Synthesis of the new complexes

2.4.1. [RuCp(PPh_3)$_2$(1-BI)][CF_3SO_3] (**1**)

To a stirred suspension of 0.320 g (0.5 mmol) of [RuCp(PPh_3)$_2$Cl] in methanol (25 mL) was added 0.090 g (0.6 mmol) of 1-benzilimidazole, followed by addition of 0.160 g (0.6 mmol) $AgCF_3SO_3$. After a 2 h reflux the colour changed from orange to yellow. The reaction mixture was cooled to room temperature and the solvent of the filtered solution was removed under vacuum; the residue was washed with n-hexane (2×10 mL) and diethyl ether (2×10 mL). Yellow crystals were obtained after recrystalization from dichloromethane/diethyl ether. Yield: 79%. ^{1}H NMR [$(CD_3)_2CO$, Me_4Si, δ/ppm, m = multiplet, d = doublet, s = singlet]: 7.50 [m, 6H, $H_{para}(PPh_3)$], 7.30 [m, 17H, $H_6+H_7+H_{meta}(PPh_3)$], 7.05 [m, 12H, $H_{orto}(PPh_3)$], 6.91 [d, 2 H, H_3+H_2, J_{2-3} = 4.25], 6.82 [s, 1H, H_1], 4.87 [s, 2H, H_4 (CH_2)], 4.56 [s, 5H, $^5\eta$-C_5H_5]. ^{13}C NMR [$(CD_3)_2CO$, δ/ppm]: 144.36 (C_1), 135.10 (C_q, PPh_3), 131.59 (CH, PPh_3), 130.52 (CH, PPh_3), 129.97–129.82 ($C_5+C_6+C_7$), 129.55 (C_3+C_2), 122.80 (CH, PPh_3), 84.21 ($^5\eta$-C_5H_5), 52.81 (C_4). ^{31}P NMR [$(CD_3)_2CO$, δ/ppm]: 42.14 (s, PPh_3). FT-IR [KBr, cm^{-1}, w = weak, m = medium, s = strong, vs = very strong]: 3135 (w), 3057 (m), 1586 (w), 1524 (m), 1479 (m), 1433 (m), 1264 (vs), 1223 (s), 1153 (s), 1088 (s), 1027 (s), 997 (m), 836 (m), 755 (m), 689 (s), 635 (s), 571 (m), 511 (s). Elemental analysis (%) found: C, 61.68; H, 4.48; N, 2.73; S, 3.11. Calc. for $C_{52}H_{45}N_2SP_2F_3O_3Ru\cdot 0.3CH_2Cl_2$ (1023.49): C, 61.38; H, 4.49; N, 2.74; S, 3.13. UV/Vis (CH_2Cl_2) λ_{max}/nm (ε/M^{-1} cm^{-1}): 359 (4392).

2.4.2. [RuCp(PPh_3)(2,2′-bipy)][CF_3SO_3] (**2**)

To a stirred suspension of 0.320 g (0.5 mmol) of [RuCp(PPh_3)$_2$Cl] in methanol (25 mL) was added 0.100 g (0.6 mmol) of 2,2′-bipyridyl,

followed by addition of 0.160 g (0.6 mmol) $AgCF_3SO_3$. After a 4 h reflux the orange colour turned out red. The reaction mixture was cooled to room temperature, filtered and the solvent was removed under vacuum; the residue was washed with n-hexane (3×10 mL) giving red crystals after recrystalization from dichloromethane/diethyl ether. Yield: 85%. ^{1}H NMR [$(CD_3)_2CO$, Me_4Si, δ/ppm, m = multiplet, d = doublet, s = singlet]: 9.48 [d, 2H, H_4]; 8.15 [d, 2H, H_1], 7.86 [t, 2H, H_2], 7.38 [m, 3H, $H_{para}(PPh_3)$], 7.30 [m, 7H, $H_3 + H_{meta}(PPh_3)$], 7.10–7.06 [m, 6H, $H_{orto}(PPh_3)$], 4.88 [s, 5H, $^5\eta$-C_5H_5]. ^{13}C NMR [$(CD_3)_2CO$, δ/ppm]: 155.23 (C_4), 135.85 (C_2), 132.39–132.28 (C_q, PPh_3), 130.99 (C_5), 130 (C_3), 129.92 (CH, PPh_3), 128.26–128.16 (CH, PPh_3), 124.76 (CH, PPh_3), 123.20 (C_1), 78.05 ($^5\eta$-C_5H_5). ^{31}P NMR [$(CD_3)_2CO$, δ/ppm]: 50.67 (s, PPh_3). FT-IR [KBr, cm^{-1}, w = weak, m = medium, s = strong, vs = very strong]: 3075 (m), 1994 (w), 1837 (w), 1630 (m), 1603 (m), 1480 (m), 1438 (s), 1309 (w), 1260 (s), 1226 (vs), 1158 (s), 1090 (m), 1029 (s), 997 (m), 836 (m), 767 (m), 637 (s), 571 (m), 513 (s), 494 (m). Elemental analysis (%) found: C, 55.66; H, 3.85; N, 3.82; S, 4.37. Calc. for $C_{34}H_{28}N_2SPF_3O_3Ru$ (734.06): C, 55.49; H, 3.77; N, 3.76; S, 4,57. UV/Vis (CH_2Cl_2) λ_{max}/nm (ε/M^{-1} cm^{-1}): 419.5 (6229).

2.4.3. [RuCp(PPh$_3$)$_2$(4-Mpy)][CF$_3$SO$_3$] (3)

To a stirred solution of 0.310 g (0.5 mmol) of [RuCp$(PPh_3)_2$Cl] in dichloromethane (25 mL) was added 0.060 mL (0.6 mmol) of 4-methylpyridine, followed by addition of 0.150 g (0.6 mmol) $AgCF_3SO_3$. After a 3 h reflux the orange colour turned out yellow. The reaction mixture was cooled to room temperature and the solvent of the filtered solution was removed under vacuum; the residue was washed with n-hexane (2×10 mL). Yellow crystals were obtained after recrystalization from dichloromethane/diethyl ether. Yield: 77%. ^{1}H NMR [$CDCl_3$, Me_4Si, δ/ppm, m = multiplet, d = doublet, s = singlet]: 8.13 [d, 2H, H_2, $J_{2,1} = 1.6$], 7.38 [m, 6H, $H_{para}(PPh_3)$], 7.25 [m, 12H, $H_{meta}(PPh_3)$], 7.05 [m, 12H, $H_{orto}(PPh_3)$], 6.57 [d, 2H, H_1], 4.46 [s, 5H, $^5\eta$-C_5H_5], 2.14 [s, 3H, $H(CH_3)$]. ^{13}C NMR [$CDCl_3$, δ/ppm]: 157.67 (C_1), 148.68 (C_3), 135.44 (C_q, PPh_3), 130.80 (CH, PPh_3), 130.30 (CH, PPh_3), 128.47 (CH, PPh_3), 126.13 (C_2), 83.51 ($^5\eta$-C_5H_5), 20.80 [$C(CH_3)$]. ^{31}P NMR [$CDCl_3$, δ/ppm]: 42.39 (s, PPh_3). FT-IR [KBr, cm^{-1}, w = weak, m = medium, s = strong, vs = very strong]: 3118 (w), 3057 (m), 2986 (w), 2920 (w), 2854 (w), 2303 (w), 1967 (w), 1899 (w), 1821 (w), 1777 (w), 1675 (w), 1617 (m), 1479 (m), 1433 (s), 1259 (vs), 1147 (s), 1088 (m), 1029 (vs), 998 (m), 920 (w), 842 (m), 814 (m), 761 (s), 745 (s) 698 (vs), 636 (s), 572 (m), 514 (s), 416 (m). Elemental analysis (%) found: C, 58.36; H, 4.34; N, 1.49; S, 3.28. Calc. for $C_{48}H_{42}NSP_2F_3O_3Ru \cdot 0.8CH_2Cl_2$ (973.54): C, 58.56; H, 4.39; N, 1.40; S, 3.20. UV/Vis (CH_2Cl_2) λ_{max}/nm (ε/M^{-1} cm^{-1}): 342.5 (2586).

2.4.4. [RuCp(dppe)(4-Mpy)][CF$_3$SO$_3$] (4)

To a stirred solution of 0.300 g (0.5 mmol) of [RuCp(dppe)Cl] in dichloromethane (20 mL) was added 0.060 mL (0.6 mmol) of 4-methylpyridine, followed by addition of 0.150 g (0.6 mmol) $AgCF_3SO_3$. After a 3 h reflux, the yellow mixture was cooled to room temperature and the solvent of the filtered solution was removed under vacuum; the residue was washed with n-hexane (3×10 mL). Yellow crystals were obtained after recrystalization from dichloromethane/diethyl ether. This compound revealed to be very sensitive to air and temperature decomposing at ~60 °C. Yield: 83%. ^{1}H NMR [$CDCl_3$, Me_4Si, δ/ppm, m = multiplet, d = doublet, s = singlet]: 7.45–7.21 [m, 22H, $H_2 + C_6H_5$ (dppe), $J_{2,1} = 1.1$], 6.26 [d, 2H, H_1], 4.61 [s, 5H, $^5\eta$-C_5H_5], 2.77 [m, 4H, CH_2 (dppe)], 1.98 [s, 3H, $H(CH_3)$]. ^{13}C NMR [$CDCl_3$, δ/ppm]: 132.15 (Cq, dppe), 130.29 (CH, dppe), 129.79 (C_2), 128.61 (CH, dppe), 125.76 (CH, dppe), 125.29 (C_1), 121.71 (C_3), 82.49 ($^5\eta$-C_5H_5), 21.00 (CH_2, dppe), 19.99 [$C(CH_3)$]. ^{31}P NMR [$CDCl_3$, δ/ppm]: 82.79 (s, dppe). FT-IR [KBr, cm^{-1}, w = weak, m = medium, s = strong, vs = very strong]: 3048 (m), 2965 (w), 2929 (w), 2290 (w), 1619 (m), 1433 (m), 1265 (vs), 1154 (s), 1100 (s), 1030 (s), 875 (m), 801 (m), 749 (m), 698 (s), 636 (s), 571 (m), 522 (s), 441 (m). UV/Vis (CH_2Cl_2) λ_{max}/nm (ε/M^{-1} cm^{-1}): 348 (2608).

2.5. Crystal structure determination

The crystal data, data collection, and refinement parameters for the X-ray structures are listed in Table 1. Data were collected for **1** on an Enraf–Nonius CAD4 four-circle diffractometer. Unit-cell parameters were determined from 25 reflections ($12 < \theta < 21°$) and refined by least-squares methods. Intensities were collected with graphite monochromatized Mo Kα radiation, using ω/2θ scan-technique; 14,546 reflections were measured in the range $2.01 \le \theta \le 29.97$, and 8510 reflections were assumed as observed applying the condition $I > 2\sigma(I)$. Lorentz-polarization and absorption corrections were made.

The structure of **1** was solved by direct methods, using SIR97 [25] computer program, and refined by full-matrix least-squares method with SHELX97 [26] computer program, using 14,546 reflections, (very negative intensities were not assumed). The function minimized was $\sum w\,||Fo|^2 - |Fc|^2|^2$, where $w = [\sigma^2(I) + (0.0465P)^2]^{-1}$, and $P = (|Fo|^2 + 2|Fc|^2)/3$, f, f′ and f″ were taken from International Tables of X-Ray Crystallography [27]. All H atoms were computed and refined, using a riding model, with an isotropic temperature factor equal to 1.2 times the equivalent temperature factor of the atom that is linked. The final R(on F) factor was 0.034, wR(on $|F|^2$) = 0.099 and goodness of fit = 0.906 for all observed reflections. Number of refined parameters was 563. Max. shift/esd = 0.00, mean shift/esd = 0.00. Max. and min. peaks in final difference synthesis was 0.696 and −0.606 eÅ^{-3}, respectively.

Data were collected for **2**, **3**, and **4** on a MAR345 diffractometer with image plate detector. Unit-cell parameters were determined from 264, 990, and 3771 reflections ($3 < \theta < 31°$) for **2**, **3**, and **4** respectively, and refined by least-squares methods. Intensities were collected with graphite monochromatized Mo Kα radiation. For **2**, 38,118 reflections were measured in the range $2.66 \le \theta \le 32.50$, 11,225 of which were non-equivalent by symmetry (R_{int}(on I) = 0.06); 7991 reflections were assumed as observed applying the condition $I > 2\sigma(I)$. Lorentz-polarization and absorption corrections were made. For **3**, 21,370 reflections were measured in the range $2.64 \le \theta \le 31.99$; 9925 of which were non-equivalent by symmetry (R_{int}(on I) = 0.077); 8401 reflections were assumed as observed applying the condition $I > 2\sigma(I)$. Lorentz-polarization but no absorption corrections were made. For **4**, 29,410 reflections were measured in the range $2.66 \le \theta \le 32.43$; 9887 of which were non-equivalent by symmetry (R_{int}(on I) = 0.053); 7826 reflections were assumed as observed applying the condition $I > 2\sigma(I)$. Lorentz-polarization and absorption corrections were made.

The structures of **2**, **3** and **4** were solved by Direct methods, using SHELXS [26] computer program, and refined by full-matrix least-squares method with SHELX97 [26] computer program. For **2**, the function minimized was $\sum w\,||Fo|^2 - |Fc|^2|^2$, where $w = [\sigma^2(I) + (0.0303P)^2]^{-1}$, and $P = (|Fo|^2 + 2|Fc|^2)/3$, f, f′ and f″ were taken from International Tables of X-Ray Crystallography [27]. All H atoms were computed and refined, using a riding model, with an isotropic temperature factor equal to 1.2 times the equivalent temperature factor of the atom that is linked. The final R(on F) factor was 0.067, wR(on $|F|^2$) = 0.920 and goodness of fit = 0.987 for all observed reflections. Number of refined parameters was 406. Max. shift/esd = 0.00, mean shift/esd = 0.00. Max. and min. peaks in final difference synthesis was 0.392 and −0.409 eÅ^{-3}, respectively. For **3** the function minimized was $\sum w||Fo|^2 - |Fc|^2|^2$, where $w = [\sigma^2(I) + (0.1681P)^2 + 0.5436P]^{-1}$, and $P = (|Fo|^2 + 2|Fc|^2)/3$, f, f′ and f″ were taken from International Tables of X-Ray Crystallography [27]. All H atoms were computed and refined, using a riding model, with an isotropic temperature factor equal to 1.2 times the equivalent temperature factor of the atom that is linked. The final R(on F) factor was 0.078, wR(on $|F|^2$) = 0.229 and goodness of fit = 1.062 for all observed reflections. Number of refined parameters was 551. Max. shift/esd = 0.00, mean shift/esd = 0.00. Max. and min. peaks in final difference synthesis was 0.785 and −0.641 eÅ^{-3}, respectively. For **4**

Table 1
Data collection and structure refinement parameters for compounds **1**.CH_2Cl_2–**4**.

Chemical formula	$C_{53}H_{47}Cl_2F_3N_2O_3P_2RuS$	$C_{34}H_{28}F_3N_2O_3PRuS$	$C_{48}H_{46}F_3NO_5P_2RuS$	$C_{38}H_{36}F_3NO_3P_2RuS$
Molecular weight	1082.90	733.68	968.93	806.75
T (K)	293(2)	293(2)	293(2)	293(2)
Wavelength	0.71073 Å	0.71073 Å	0.71073 Å	0.71073 Å
Crystal system	Triclinic	Monoclinic	Monoclinic	Monoclinic
Space group	$P\bar{1}$	$P2_1/c$	$P2_1/n$	$P2_1/c$
a (Å)	11.548(4)	11.402(5)	11.310(5)	11.044(4)
b (Å)	14.642(9)	16.883(5)	32.539(11)	12.717(4)
c (Å)	16.303(7)	16.536(5)	12.987(3)	25.933(6)
α (°)	83.21(4)	90	90	90
β (°)	77.65(3)	99.69(2)	103.73(2)	99.95(2)
γ (°)	68.43(4)	90	90	90
V(Å^3)	2502(2)	3137.8(19)	4643(3)	3587.4(19)
Z	2	4	4	4
D_c (g cm^{-3})	1.437	1.553	1.386	1.494
Absorp. Coeff. (mm^{-1})	0.582	0.673	0.509	0.638
Final R indices [I>2σ(I)]	$R_1 = 0.0341$	$R_1 = 0.0311$	$R_1 = 0.0744$	$R_1 = 0.0481$
R índices (all data)	$R_1 = 0.0921$	$R_1 = 0.0479$	$R_1 = 0.0788$	$R_1 = 0.0651$

the function minimized was $\sum w||Fo|^2 - |Fc|^2|^2$, where $w = [\sigma^2(I) + (0.0781P)^2 + 0.2671P]^{-1}$, and $P = (|Fo|^2 + 2|Fc|^2)/3$, f, f′ and f″ were taken from International Tables of X-Ray Crystallography [27]. All H atoms were computed and refined, using a riding model, with an isotropic temperature factor equal to 1.2 times the equivalent temperature factor of the atom that is linked. The final R(on F) factor was 0.048, wR(on $|F|^2$) = 0.142 and goodness of fit = 1.126 for all observed reflections. Number of refined parameters was 442. Max. shift/esd = 0.00, mean shift/esd = 0.00. Max. and min. peaks in final difference synthesis was 0.707 and −0.970 eÅ^{-3}, respectively.

CCDC 763263–763266 contain the supplementary crystallographic data for this paper. These data can be obtained free of charge from the Cambridge Crystallographic Data Centre via https://www.ccdc.cam.ac.uk/services/structure_deposit/.

2.6. Electrochemical experiments

The electrochemical experiments were performed on an EG&G Princeton Applied Research Model 273A potentiostat/galvanostat and monitored with a personal computer loaded with Electrochemistry PowerSuite v2.51 software from Princeton Applied Research. Cyclic voltammograms were obtained in 0.1 M solutions of [NBu_4][PF_6] in CH_2Cl_2 or CH_3CN, using a three-electrode configuration with a platinum-disk working electrode (1.0 mm diameter), a silver-wire pseudo-reference electrode and a Pt wire auxiliary electrode. The electrochemical experiments were performed under a N_2 atmosphere at room temperature. The redox potentials of the complexes were measured in the presence of ferrocene as the internal standard and the redox potential values are normally quoted relative to the SCE (saturated calomel electrode) by using the ferrocenium/ferrocene redox couple ($E_{p/2} = 0.46$ or 0.40 V vs SCE for CH_2Cl_2 or CH_3CN, respectively) [28].

The supporting electrolyte was purchased from Aldrich Chemical Co., recrystallized from ethanol, washed with diethyl ether and dried under vacuum at 110 °C for 24 h. Reagent grade acetonitrile and dichloromethane were dried over P_2O_5 and CaH_2, respectively, and distilled under nitrogen atmosphere before use.

3. Results and discussion

3.1. Synthesis

The four new cationic complexes of ruthenium (II) of the type [Ru(η^5-C_5H_5)(PP)L][CF_3SO_3] with PP = 2PPh_3 or dppe were prepared by σ coordination of the nitrogen atom of the L heteroaromatic ligands 1-benzylimidazole (1-BI), 2,2′-bipyriyl (2,2′-bipy) and 4-methylpyridine (4-Mpy). The structures of these new compounds were also characterized by X-ray diffraction studies (see later discussion). Compounds were obtained in good yields, by halide abstraction from [Ru(η^5-C_5H_5)(PP)Cl] with silver triflate, refluxing several hours in dichloromethane or methanol (Scheme 1) and recrystallized of dichloromethane/diethyl ether. The new compounds were fully characterized by FT-IR, ^{1}H, ^{13}C and ^{31}P NMR spectroscopies; the elemental analyses were in accordance with the proposed formulations.

3.2. NMR spectroscopic studies

^{1}H NMR resonances for the cyclopentadienyl ring are in the characteristic range of monocationic ruthenium(II) complexes. The effect of coordination of the N heteroaromatic ligands is observed through the shielding on the protons of the coordinating ring, which is remarkably for H_1 proton, adjacent to the coordinated N atom, indicating an electronic flow towards the aromatic ligand due to π-backdonation involving the metal centre. This effect is very pronounced in the compound **4**, where the observed shielding was of 2.37 ppm, showing also the better σ-donor ability of dppe compared to PPh_3 coligand. The observed shieldings on compounds **3**, **1** and **2** were 2.06, 0.86 and 0.44 ppm, respectively. Table 2 presents the ^{1}H NMR chemical shifts of the free and coordinated ligands. The spectra are collected in Figures S1–S4 in Supplementary Material.

^{13}C NMR spectra revealed the same general effect of shielding observed for the protons.

^{31}P NMR data of the complexes showed a single sharp signal for the phosphine coligands (dppe and PPh_3) revealing the equivalency of the two phosphorus atoms, and an expected deshielding upon coordination, in accordance with its σ donor character.

3.3. X-ray structural studies of the complexes

Suitable crystals for X-ray diffraction studies were obtained for all the new compounds using the same crystallization slow diffusion method. All the compounds crystallized in centrosymmetric space group. Compound **1** crystallized in triclinic crystal system and compounds **2**, **3** and **4** in monoclinic crystal system.

The molecular structures of the compounds [Ru(η5-C_5H_5)(PPh_3)$_2$(1-BI)][CF_3SO_3] **1** and [Ru(η^5-C_5H_5)(dppe)(4-Mpy)][CF_3SO_3] **4** are respectively presented in Figs. 1 and 2. The molecular structures of compounds **2** and **3** are collected in Figures S5–S6 in Supplementary Material. All the structures consist in "piano stool" distribution formed by the ruthenium-Cp unit bound to the phosphines and nitrogen ligand. In Table 3, selected bond lengths and angles for compounds **1.**CH_2Cl_2, **2**, **3** and **4** are collected. The distances of ruthenium atom and

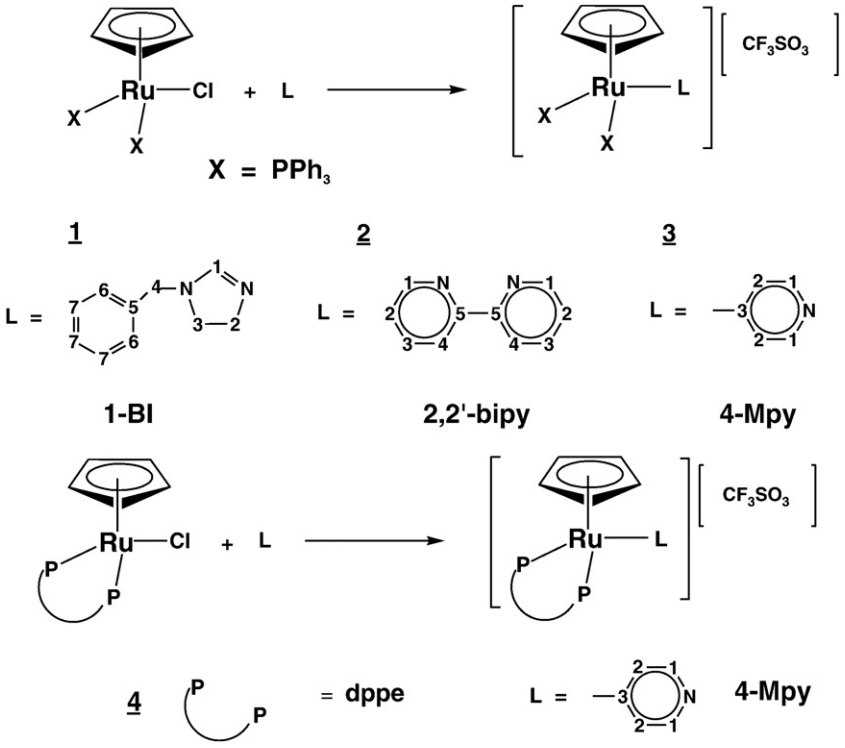

Scheme 1. Reaction scheme for the synthesis of the complexes $[Ru(\eta^5C_5H_5)(PPh_3)_2\,L][CF_3SO_3]$ and $[Ru(\eta^5C_5H_5)(dppe)L][CF_3SO_3]$ with ligand numbering for NMR spectra.

Cp ring are 1.851(2), 1.833(2), 1.860(2) and 1.876(2) for compounds **1**, **2**, **3** and **4** respectively, in good agreement with the donor/acceptor nature and number of other ligands bound to ruthenium atom: CpRuN(1-BI)$P_1(PPh_3)P_2(PPh_3)$ for complex **1**, $CpRuN_1N_2$(2,2′-bipy)$P_1(PPh_3)$ for complex **2**, CpRuN(4-Mpy)$P_1(PPh_3)$ $P_2(PPh_3)$ for complex **3** and CpRuN(4-Mpy)P_1P_2(dppe) for complex **4**. The shorter distance between aromatic rings for compounds **1** and **4** is higher than 4 Å, in consequence, stacking interactions can be discarded. However, the shorter distance found for two aromatic ligands in compound **2**, between the bipyridine ligand ring $N_2C_{11}C_{12}C_{13}C_{14}C_{15}$ and the phosphine phenyl ring $C_{22}C_{23}C_{24}C_{25}C_{26}C_{27}$, is 3.744(2) Å and in compound **3**, between the methylpyridine ligand ring defined by $NC_6C_7C_8C_9C_{10}$ and the phenyl ring $C_{36}C_{37}C_{38}C_{39}C_{40}C_{41}$ from one of the phosphine ligands is 3966(3) Å. These two values are in the frontier of those that are considered to establish stacking interactions.

3.4. Electrochemical studies

Looking for the elucidation of structure-activity relationships for $[Ru(\eta^5\text{-}C_5H_5)(PP)(L)]^+$ complexes, where L = nitrogen heterocycle, the redox potential can be an important parameter to determine the physiological activities of these Ru(II)-based drugs. Taking this in mind, the redox behavior of the new complexes **1234** were studied by cyclic voltammetry in dichloromethane and acetonitrile and the most relevant data are presented in Table 4 and Figures S7–S12 (supplementary data).

Table 2
Selected ^{1}H NMR data for compounds $[Ru(\eta^5\text{-}C_5H_5)(PP)L][CF_3SO_3]$ (**1234**) and the free ligands.

	H_1	H_2	H_3	H_4	H_6	H_7
1-BI	7.68 (s)	6.95 (d)	7.10 (d)	5.26 (s)	7.29 (m)	7.29 (m)
1	6.82 (s)	6.91 (d)	6.91 (d)	4.87 (s)	7.30 (m)	7.30 (m)
2,2′-bipy	8.59 (m)	7.12 (m)	7.66 (m)	8.50 (m)	–	–
2	8.15 (m)	7.86 (t)	7.30 (m)	9.48 (d)	–	–
4-Mpy	8.63 (d)	7.104 (d)	–	2.349 (s)	–	–
3	6.57 (d)	8.13 (d)	–	2.14 (s)	–	–
4	6.26 (d)	7.34 (m)	–	1.98 (s)	–	–

s = singlet, d = doublet, m = multiplet.

The electrochemical response of $[Ru(\eta^5\text{-}C_5H_5)(PPh_3)_2(1\text{-BI})][CF_3SO_3]$ (**1**) in dichloromethane is characterized by a quasi-reversible process at 0.90 V, attributed to the Ru(II)/Ru(III) redox pair, followed by a second irreversible oxidation process (1.56 V) attributed to the 1-benzilimidazole ligand (1-BI). For complex **2** $[Ru(\eta^5\text{-}C_5H_5)(PPh_3)$(2,2′-bipy)$][CF_3SO_3]$, the quasi-reversible Ru(II)/Ru(III) process at 1.05 V and two irreversible oxidation processes (E_{pa} = 1.53 and 1.70 V) were observed. Complexes **3** and **4** with 4-methylpyridine showed a consistent electrochemical behavior in dichloromethane with the quasi-reversible Ru(II)/Ru(III) redox process at potentials 1.075 and 0.91 V respectively, dependent on the phosphorus coligands.

In acetonitrile, the general behavior of the complexes is slightly different than for dichloromethane. For complex **1**, the oxidation process Ru(II)/Ru(III) became irreversible and a new redox wave was found in the negative potentials probably attributed to any process occurring at the coordinated benzylimidazole ligand. Concerning the oxidative electrochemistry of complexes **3** and **4**, the electrochemical studies in acetonitrile showed a significant difference. In fact, the CV of complex **3** showed a Ru(II)/Ru(III) oxidation at 1.23 V with no cathodic counterpart and a reductive process arises at negative potentials (−0.515 V). This later process has been attributed to decomposition products originated by the oxidative process, since it vanishes when the scan direction is reversed. Complex **4** showed a first irreversible oxidation process at 0.80 V and a second quasi-reversible process at 1.01 V. Scan rate studies on the first oxidation process, showed that it became reversible when the scan direction is reverted immediately after the oxidative potential and for high scan rates (200–1000 mV s^{-1}). This behavior can be associated to a Ru(II)/Ru(III) oxidation, followed by fast substitution of the 4-methylpyridine ligand by an acetonitrile solvent molecule, leading to the $[RuCp(dppe)(NCCH_3)]^+$ species, responsible for the appearance of the second quasi-reversible redox process. This result is consistent with our earlier studies on monocyclopentadienylruthenium(II)dppe

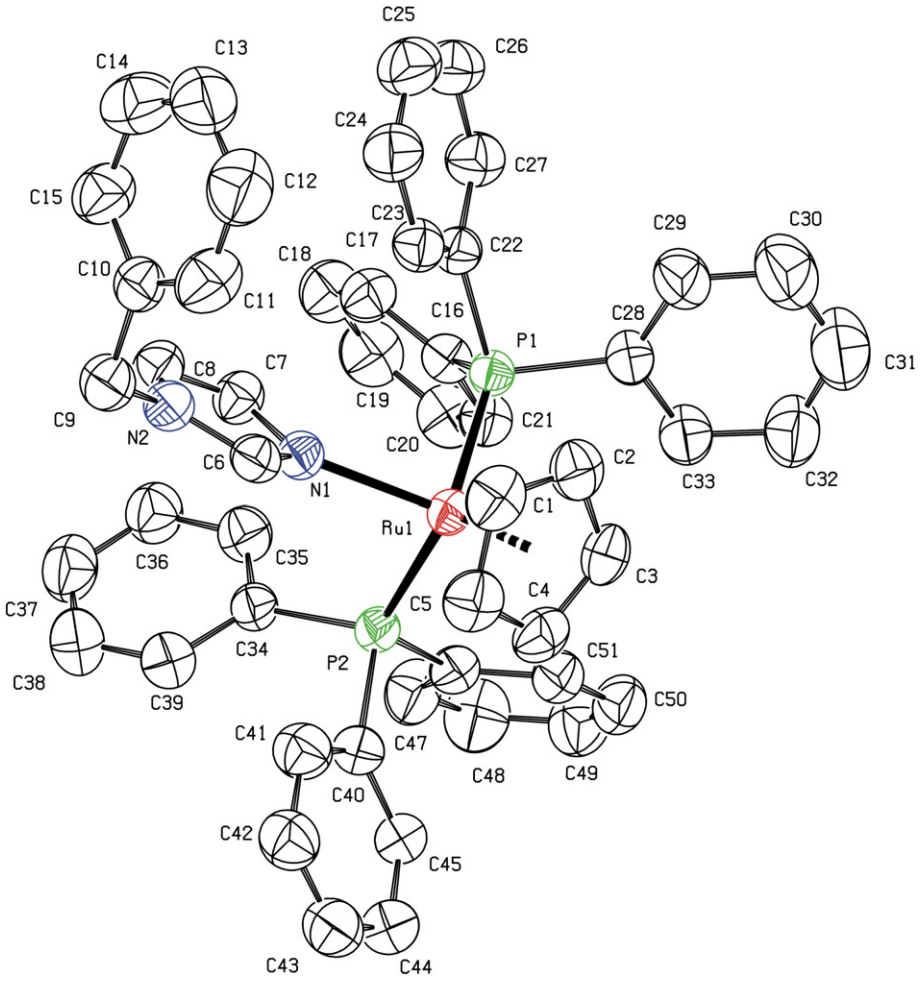

Fig. 1. ORTEP for [Ru(η^5-C_5H_5)(PPh_3)$_2$(1-BI)][CF_3SO_3] **1**.

derivatives containing thiophene ligands [29]. This characteristic propensity for ligand exchange reactions can constitute an advantage for the Ru(II) species, since it can lead to a more rapid interaction with the target biomolecules.

3.5. Electronic absorption spectroscopy

The optical absorption spectra of all the synthesized new complexes were recorded in ~10^{-4} mol dM^{-3} solutions of dichloromethane. For comparison, also the electronic spectra of the uncoordinated ligands and of the [RuCp(PP)Cl] parent compound were obtained in the same experimental conditions. All the complexes showed two intense absorption bands in the UV region, attributed to electronic transitions occurring in the organometallic fragment $[MCp(PP)]^+$ ($\lambda \approx 240$ nm) and coordinated chromophores in the range 320–380 nm. In addition to these bands, two maximum absorptions at 423 nm and 475 nm were found for compound [RuCp(PPh_3)(2,2′-bipy)][CF_3SO_3] **2**, attributed to the metal-to-ligand-charge-transfer (MLCT) transitions, from Ru 4d orbitals to the bipyridine ring π*. Figure S13 (Supplementary Material) illustrates the observed optical spectra in dichloromethane, compared to the 2,2′-bipyridyl compound and the ruthenium parent complex.

3.6. Biological studies

3.6.1. Atomic force microscopy

AFM images of free plasmid pBR322 DNA and pBR322 DNA incubated with the [RuCp(PPh_3) (2,2′-bipy)][CF_3SO_3] **2**, are shown in Fig. 3(a) and (b) respectively. In the image (b), several supercoiled forms of plasmid DNA strongly modified, could indicate interaction with DNA in a similar way than that previously observed for typical intercalating molecules like 9-aminoacridine [30,31]. The study of the variation of the viscosity of a Calf Thymus DNA solution incubated with the compound at different relationships compound/DNA shows an increasing on the viscosity which is observed when intercalation occurs. (See Supplementary Material, Figure S14). An increase in viscosity of native DNA is regarded as a diagnostic feature of an intercalation process [32,33].

Modifications caused on the free pBR322 by the complex [RuCp(PPh_3)$_2$(1-BI)][CF_3SO_3] **1** after 1 min of incubation (a) and 30 min of incubation (b) at room temperature, are shown in Figure S15 (Supplementary Material). The 1-benzylimidazole ligand or the phenyl groups of the two phosphine ligands bound to ruthenium atom (see molecular structure in Fig. 1) are capable of intercalation between base pairs of DNA.

The variation of the viscosity of Ct-DNA solution incubated for longer time (24 h) with compounds **3** and **4** with the concentration also shows the typical increase due to an intercalation process (see Supplementary Material Figures S16 and S17).

3.6.2. Cytotoxicity of the ruthenium complexes against HL-60 cells

The effect of the ruthenium complexes was examined on human leukemia cancer cells (HL-60) using the MTT assay, a colorimetric determination of cell viability during *in vitro* treatment with a drug. The assay, developed as an initial stage of drug screening, measures the amount of MTT reduction by mitochondrial dehydrogenase and assumes that cell viability (corresponding to the reductive activity) is

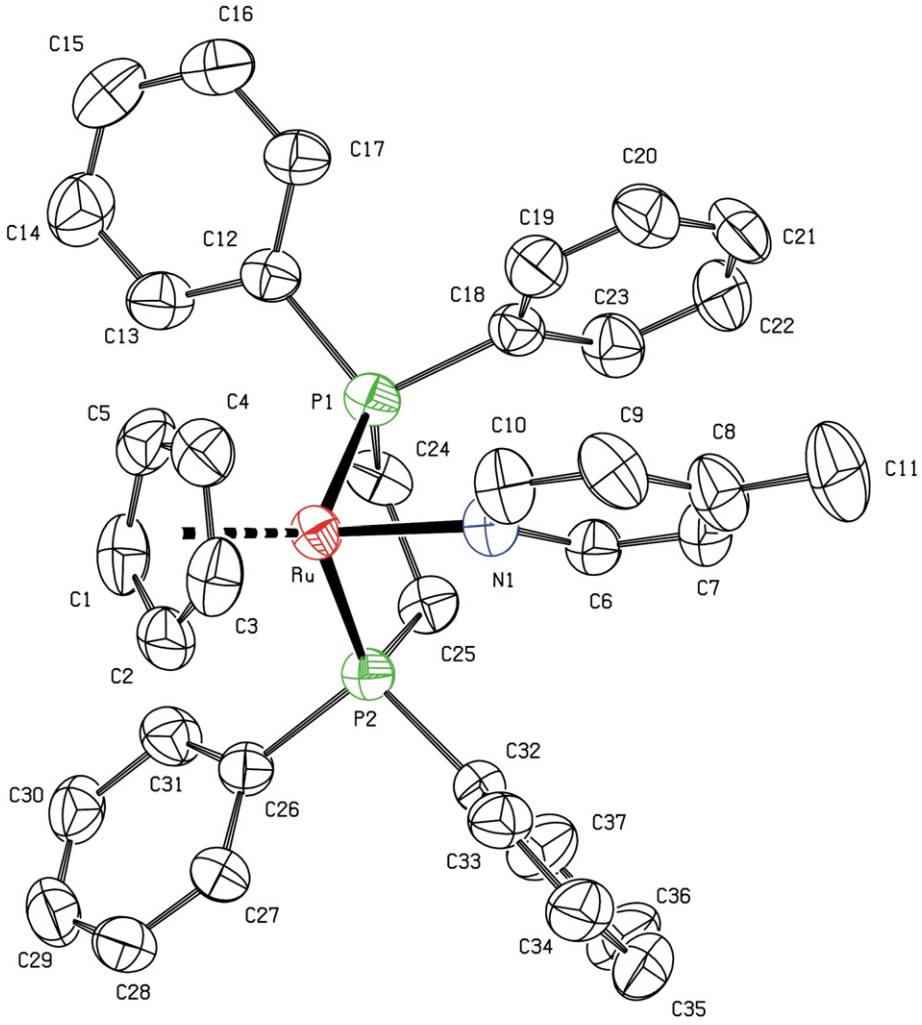

Fig. 2. ORTEP for $[Ru(\eta^5\text{-}C_5H_5)(dppe)(4\text{-}Mpy)][CF_3SO_3]$ **4**.

proportional to the production of purple formazan that is measured spectrophotometrically. A low IC_{50} is desired and implies cytotoxicity or antiproliferation at low drug concentrations.

The drugs tested in this experiment were cisplatin and compounds **1234**. Cells were exposed to each compound continuously for a 24 h or a 72 h period and then assayed for growth using the MTT endpoint. The IC_{50} values of complexes **1234** and cisplatin for the growth inhibition of HL-60 cells are shown in Table 5.

The IC_{50} value of cisplatin for growth inhibition of HL-60 cells for 24 h exposition was 15.61 ± 1.15 μM, which is greater than the values obtained for the ruthenium complexes. It was notable that complex **1** showed much higher cytotoxicity than the other three compounds. Complexes **2** and **4** were comparable and complex **3** appeared to be slightly more cytotoxic.

The cytotoxicities of the all the complexes were also determined for 72 h. As listed in Table 5, the IC_{50} for ruthenium complexes decreased until submicromolar values in some cases. Compound **1** presents the smaller values for both times 24 h or 72 h. In conclusion, all the ruthenium complexes are more cytotoxic than cisplatin against the HL-60 tumour cell line.

3.6.3. Quantification of apoptosis by Annexin V binding and flow cytometry

We have also analyzed by Annexin V-PI flow cytometry whether complexes **1234** are able to induce apoptosis in HL-60 cells after 24 h of incubation at equitoxic concentrations (IC_{50} values). All ruthenium complexes induce cell death mainly by apoptosis. The most active metal complex is complex **2**, which is able to induce a similar percentage (36%) of apoptotic death that cisplatin does it. Although the percentage of apoptotic death for complexes **1** (24%), **3** (13%) and **4** (20%) is a little smaller, it is clear that the mechanism of apoptotic death is also induced by these ruthenium compounds and this fact cannot be discarded (Supplementary Material, Table S1).

4. Conclusion

A new family of Ru(II) three-legged piano stool complexes possessing planar N heteroaromatic sigma bonded ligands, was synthesized and fully characterized. The complexes were tested for potential antitumor activity against the human promyelocytic leukemia cell line HL-60 using a MTT assay. The four complexes tested possess excellent antitumor activities, with IC_{50} values lower than that of cisplatin. Although the four complexes present promising antitumor behavior, compounds **1** and **2** have given lower values of IC_{50} at 72 h than the other complexes. This could indicate that the DNA is also for these type of ruthenium compounds one of the targets of their action inside the cells.

Supplementary materials related to this article can be found online at doi:10.1016/j.jinorgbio.2010.10.009.

Abbreviations

1-BI	1-benzylimidazole
2,2′-bipy	2,2′-bipyridyl

Table 3
Selected bond lenghts (Å) and angles (°) for compounds **1**.CH_2Cl_2–**4**.

*Compound **1**.CH2Cl2*			
Bond lengths (Å)			
Ru(1)–N(1)	2.144(3)	N(1)–C(7)	1.369(3)
Ru(1)–Cp	1.851(2)	N(2)–C(8)	1.331(4)
Ru(1)–P(1)	2.347(2)	N(2)–C(6)	1.344(4)
Ru(1)–P(2)	2.353(2)	N(2)–C(9)	1.477(4)
Bond angles (°)			
N(1)–Ru(1)–P(1)	92.61(8)	C(6)–N(1)–Ru(1)	124.04(19)
N(1)–Ru(1)–P(2)	88.31(7)	C(7)–N(1)–Ru(1)	130.72(18)
P(1)–Ru(1)–P(2)	104.94(4)	C(8)–N(2)–C(6)	107.0(2)
*Compound **2***			
Bond lengths (Å)			
Ru(1)–N(2)	2.084(2)	N(1)–C(6)	1–3533(19)
Ru(1)–N(1)	2.084(2)	N(1)–C(10)	1.3608(19)
Ru(1)–Cp	1.833(2)	N(2)–C(15)	1.3504(18)
Ru(1)–P(1)	2.322(6)	N(2)–C(11)	1.3618(189
Bond angles (°)			
N(2)–Ru(1)–N(1)	76.62(5)	C(6)–N(1)–Ru(1)	124.58(11)
N(2)–Ru(1)–P(1)	90.56(4)	C(15)–N(2)–Ru(1)	124.89(10)
N(1)–Ru(1)–P(1)	88.97(4)	C(11)–N(2)–Ru(1)	117.05(9)
*Compound **3***			
Bond lengths (Å)			
Ru(1)–N(1)	2.170(3)	Ru(1)–P(1)	2.3729(10)
Ru(1)–Cp	1.860(2)	N(1)–C(10)	1.336(4)
Ru(1)–P(2)	2.348(2)	N(1)–C(6)	1.348(5)
Bond angles (°)			
N(1)–Ru(1)–P(2)	88.13(8)	C(10)–N(1)–C(6)	116.6(3)
N(1)–Ru(1)–P(1)	92.55(8)	C(10)–N(1)–Ru(1)	122.7(2)
*Compound **4***			
Bond lengths (Å)			
Ru(1)–N(1)	2.153(2)	Ru(1)–P(1)	2.2998(9)
Ru(1)–P(2)	2.295(2)	N(1)–C(10)	1.362(4)
Bond angles (°)			
N(1)–Ru(1)–P(2)	94.01(7)	C(6)–N(1)–C(10)	114.5(3)
N(1)–Ru(1)–P(1)	90.72(7)	C(6)–N(1)–Ru(1)	125.31(19)

4-Mpy	4-methylpyridine
Im	imidazole
AFM	atomic force microscopy
Cp	η^5-cyclopentadienyl
Dppe	1,2-bis(diphenylphosphine)ethane
Pta	1,3,5-triaza-7-phosphoadamantane
MTT	3-(4,5-dimethylthiazol-2-yl)-2,5-diphenyltetrazolium bromide
SCE	saturated calomel electrode
CDDP	cis-dichlorodiammine platinum(II)

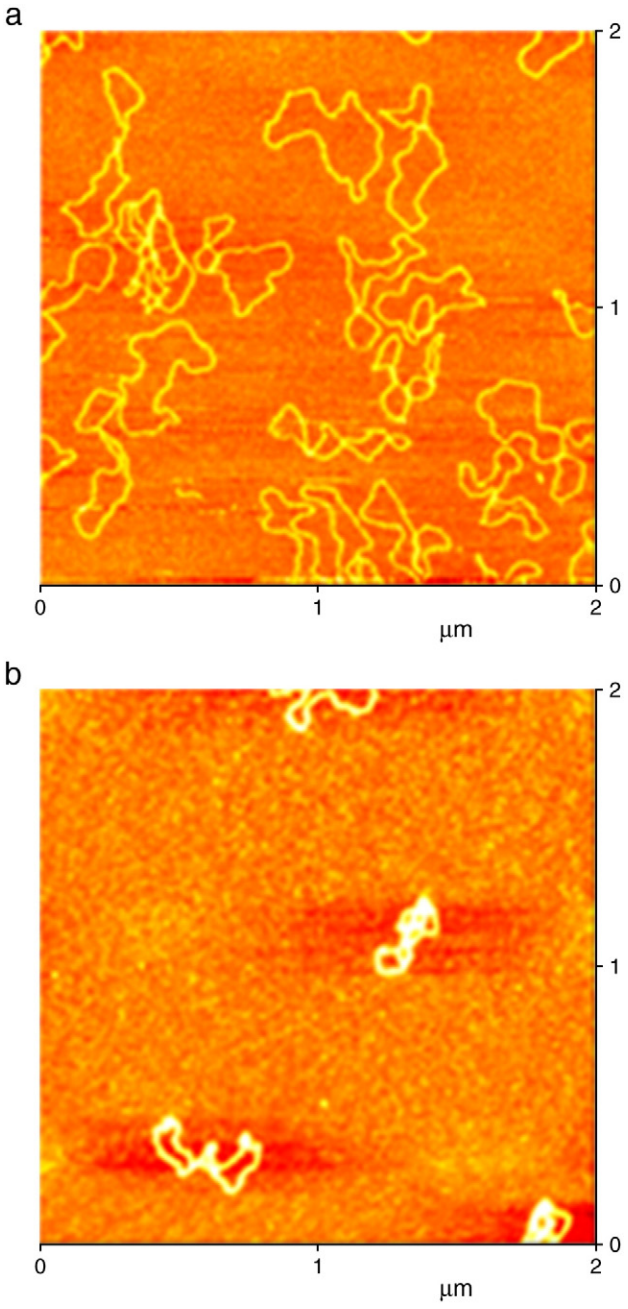

Fig. 3. AFM image of the a) free plasmid pBR322 DNA, b) plasmid pBR322 DNA incubated with the complex [RuCp(PPh_3) (2,2′-bipy)][CF_3SO_3] **2** after 1 h.

Acknowledgments

We thank to Fundação para a Ciência e Tecnologia for financial support (PTDC/QUI/66148/2006) and Ministerio de Ciencia e Innovación de España for financial support (CTQ2008-02064) and BIO2007-6846-C02-01. Tânia Morais thanks FCT for her Ph.D Grant (SFRH/BD/45871/

Table 4
Selected electrochemical data for complexes [Ru(η^5–C_5H_5)(PP)L][CF_3SO_3] (**1234**) in acetonitrile and dichloromethane at scan rate of 200 mV s^{-1}.

Complex	$E_{p/2}$ (Ru^{II}/Ru^{III}) (V), (ΔE)	Ep $_{ligand\ oxid\ or\ red}$ (V)	Solvent
[Ru(η^5-Cp)(PPh_3)$_2$(BI)]$^+$ (**1**)	0.90 (80)	1.56	CH_2Cl_2
	0.89[a]	1.18 (Ep_a); –0.68 (Ep_c)	CH_3CN
[Ru(η^5-Cp)(PPh_3)$_2$(2,2′-bipy)]$^+$ (**2**)	1.05 (90)	1.53 (Ep_a); 1.70 (Ep_a)	CH_2Cl_2
	0.88 (80)	–	CH_3CN
[Ru(η^5-Cp)(PPh_3)$_2$(4-MePy)]$^+$ (**3**)	1.075 (110)	–	CH_2Cl_2
	1.23[a]	–	CH_3CN
[Ru(η^5-Cp)(dppe)(4-Mepy)]$^+$ (**4**)	0.91 (100)	–	CH_2Cl_2
	0.80 (60)	–	CH_3CN

[a] Ep_a value. Irreversible processes.

Table 5
IC_{50} values of ruthenium compounds, and cisplatin against HL-60 cells.

complex	IC_{50} (μM)	IC_{50} (μM)
	72 h	24 h
$[RuCp(PPh_3)_2(1\text{-BI})][CF_3SO_3]$ **1**	0.38 ± 0.14	0.62 ± 0.37
$[RuCp(PPh_3)(2,2'\text{-bipy})][CF_3SO_3]$ **2**	0.42 ± 0.25	3.30 ± 0.83
$[RuCp(PPh_3)_2(4\text{-Mpy})][CF_3SO_3]$ **3**	1.06 ± 0.12	1.54 ± 0.72
$[RuCp(dppe)(4\text{-Mpy})][CF_3SO_3]$ **4**	0.92 ± 0.29	2.49 ± 1.29
CDDP	2.15 ± 0.1	15.61 ± 1.15

2008). We thank Dra. Maria J. Prieto (AFM facilities), Ibis Colmenares (viscosity measurements), Dra. Francisca García, Francisco Cortés and Manuela Costa (SCAC-Cell Culture, Antibody Production and Cytometry Facility) for technical assistance.

References

[1] A.C.G. Hotze, S.E. Caspers, D. de Vos, H. Kooijman, A.L. Spek, A. Flamigni, M. Bacac, G. Sava, J.G. Haasnoot, J. Reedijk, J. Biol. Inorg. Chem. 9 (2004) 354–364.
[2] R.A. Vilaplana, F. Delmani, C. Manteca, J. Torreblanca, J. Moreno, G. García Herdugo, F. González-Vilchez, J. Inorg. Biochem. 100 (2006) 1834–1841.
[3] A. Habtemariam, M. Melchart, R. Fernandez, S. Parsons, I.D.H. Oswald, A. Parkin, F.P.A. Fabbiani, J.E. Davidson, A. Dawson, R.E. Aird, D.I. Jodrell, P.J. Sadler, J. Med. Chem. 49 (2006) 6858–6868.
[4] G. Sava, S. Pacor, A. Bergamo, M. Cocchietto, G. Mestroni, E. Alessio, Chem. Biol. Interact. 95 (1995) 109–126.
[5] C.G. Hartinger, S. Zorbas-Seifried, M.A. Jakupec, B. Kynast, H. Zorbas, B.K. Keppler, J. Inorg. Biochem. 100 (2006) 891–904.
[6] A. Vacca, M. Bruno, A. Boccarelli, M. Coluccia, D. Ribatti, A. Bergamo, S. Garbisa, L. Sartor, L.G. Sava, Br. J. Cancer 86 (2002) 993–998.
[7] G. Pintus, B. Tadolini, A.M. Posadino, B. Sanna, M. Debidda, F. Bennardini, G. Sava, C. Ventura, Eur. J. Biochem. 269 (2002) 5861–5870.
[8] G. Sava, F. Frausin, M. Cocchietto, F. Vita, E. Podda, P. Spessotto, A. Furlani, V. Scarcia, G. Zabucchi, Eur. J. Cancer 40 (2004) 1383–1396.
[9] I. Khalaila, A. Bergamo, F. Bussy, G. Sava, P.J. Dyson, Int. J. Oncol. 29 (2006) 261–268.
[10] W.H. Wang, P.J. Dyson, Eur. J. Inorg. Chem. (2006) 4003–4018.
[11] R.E. Aird, J. Cummings, A.A. Ritchie, M. Muir, R.E. Morris, H. Chen, P.J. Sadler, D.I. Jodrell, Br. J. Cancer 86 (2002) 1652–1657.
[12] C.S. Allardyce, P.J. Dyson, D.J. Ellis, S.L. Heath, Chem. Commun. (2001) 1396–1397.
[13] L.A. Huxham, E.L.S. Cheu, B.O. Patrick, B.R. James, Inorg. Chim. Acta 352 (2003) 238–246.
[14] R.E. Morris, R.E. Arid, P.S. Murdoch, H. Chen, J. Cummings, N.D. Hughes, S. Parsons, A. Parkin, G. Boyd, D.I. Jodrell, P.J. Sadler, J. Med. Chem. 44 (2001) 3616–3621.
[15] A.H. Velders, H. Kooijman, A.L. Spek, J.G. Haasnoot, D. de Vos, J. Reedijk, Inorg. Chem. 39 (2000) 2966–2967.
[16] C.A. Vock, W.H. Ang, C. Scolaro, A.D. Phillips, L. Lagopoulos, L. Juillerat-Jeanneret, G. Sava, R. Scopelliti, P. Dyson, J. Med. Chem. 50 (2007) 2166–2175.
[17] E. Meggers, G.E. Atilla-Gokcumen, H. Bregman, J. Maksimoska, S.P. Mulkahy, N. Pagano, D.S. Williams, Synlett (2007) 1177–1189.
[18] M.H. Garcia, T.S. Morais, P. Florindo, M.F.M. Piedade, V. Moreno, C. Ciudad, V. Noe, J. Inorg. Biochem. 103 (2009) 354–361.
[19] V. Moreno, J. Lorenzo, F.X. Aviles, M.H. Garcia, J.P. Ribeiro, T.S. Morais, P. Florindo, M.P. Robalo, Bioinorg. Chem. Appl. (2010) 1–11, doi:10.1155/2010/936834.
[20] D.D. Perrin, W.L.F. Amarego, D.R. Perrin, Purification of Laboratory Chemicals, 2nd Ed., Pergamon, New York, 1980, pp. 65–371.
[21] M.I. Bruce, N.J. Windsor, Aust. J. Chem. 30 (1977) 1601–1604.
[22] T. Mosmann, J. Immunol. Methods 65 (1983) 55–63.
[23] I. Vermes, C. Haanen, H. Steffens-Nakken, C. Reutelingsperger, J. Immunol. Methods 184 (1995) 39–51.
[24] G.S. Ashby, M.I. Bruce, I.B. Tomkins, R.C. Walli, Aust. J. Chem. 32 (1979) 1003–1016.
[25] A. Altomare, M.C. Burla, M. Camalli, G. Cascarano, G. Giocovazzo, A. Guagliardi, A.G.G. Moliterini, G. Polidoro, R. Spagna, J. Appl. Crystallogr. 32 (1999) 115–119.
[26] G.M. Sheldrick, SHELXL-97: Program for the Refinement of Crystal Structure, University of Gottingen, Germany, 1997.
[27] International Tables of X-Ray Crystallography; Kynoch Press, Birmingham, IV (1974) 99–100 and 149.
[28] N.G. Conelly, W.E. Geiger, Chem. Rev. 96 (1996) 877–910.
[29] M.H. Garcia, P.J. Mendes, M.P. Robalo, M.T. Duarte, N. Lopes, J. Organomet. Chem. 694 (2009) 2888–2897.
[30] X. Riera, V. Moreno, C.J. Ciudad, V. Noe, M. Font-Bardía, X. Solans, Bioinorg. Chem. Appl. (2007) 1–15, doi:10.1155/2007/98732.
[31] J. Ruiz, J. Lorenzo, C. Vicente, G. López, J.M. López de Luzuriaga, M. Monge, F.X. Avilés, D. Bautista, V. Moreno, M. Laguna, Inorg. Chem. 47 (2008) 6990–7001.
[32] S.I. Mee, A. Pierre, J. Markovits, G. Atassi, A.J. Sablon, J.M. Saucler, Mol. Pharmacol. 53 (1998) 213–220.
[33] M.S. Shahabuddin, M. Gopal, S.C. Raghavan, J. Cancer Mol. 3 (2007) 139–146.